Oncogene (2014), 1–12

www.nature.com/onc

ORIGINAL ARTICLE

RSUME inhibits VHL and regulates its tumor suppressor function

J Gerez[1,2,5], L Tedesco[1,5], JJ Bonfiglio[1,2], M Fuertes[1], M Barontini[3], S Silberstein[1,2], Y Wu[4], U Renner[4], M Páez-Pereda[4], F Holsboer[4], GK Stalla[4] and E Arzt[1,2]

Somatic mutations or loss of von Hippel–Lindau (pVHL) happen in the majority of VHL disease tumors, which present a constitutively active Hypoxia Inducible Factor (HIF), essential for tumor growth. Recently described mechanisms for pVHL modulation shed light on the open question of the HIF/pVHL pathway regulation. The aim of the present study was to determine the molecular mechanism by which RSUME stabilizes HIFs, by studying RSUME effect on pVHL function and to determine the role of RSUME on pVHL-related tumor progression. We determined that RSUME sumoylates and physically interacts with pVHL and negatively regulates the assembly of the complex between pVHL, Elongins and Cullins (ECV), inhibiting HIF-1 and 2α ubiquitination and degradation. We found that RSUME is expressed in human VHL tumors (renal clear-cell carcinoma (RCC), pheochromocytoma and hemangioblastoma) and by overexpressing or silencing RSUME in a pVHL-HIF-oxygen-dependent degradation stability reporter assay, we determined that RSUME is necessary for the loss of function of type 2 pVHL mutants. The functional RSUME/pVHL interaction in VHL-related tumor progression was further confirmed using a xenograft assay in nude mice. RCC clones, in which RSUME was knocked down and express either pVHL wt or type 2 mutation, have an impaired tumor growth, as well as HIF-2α, vascular endothelial growth factor A and tumor vascularization diminution. This work shows a novel mechanism for VHL tumor progression and presents a new mechanism and factor for targeting tumor-related pathologies with pVHL/HIF altered function.

Oncogene advance online publication, 15 December 2014; doi:10.1038/onc.2014.407

INTRODUCTION

Originally isolated from highly tumorigenic and angiogenic cells, the product of the *RWDD3* gene, RSUME (RWD domain-containing protein SUMO Enhancer), increases protein sumoylation,[1] a dynamic post-translational modification that regulates diverse cellular processes.[2,3] RSUME is expressed in several normal tissues such as cerebellum, pituitary, kidney, pancreas, heart and adrenal gland and is induced by heat shock[4] and hypoxia (HPX).[1,5] It has been associated with other 15 genes in a breast cancer risk predictive signature[6] and in a genome-wide association study performed in 2204 breast cancer patients,[7] whereas the associated paclitaxel-induced neuropathy was not confirmed in ovarian cancer patients.[8] It has been also associated with the development of neuropathic pain[9] and with other six genes in the molecular signature of the ganglionic eminence development.[10]

Hypoxia Inducible Factors (HIFs) are heterodimeric transcription factors that induce essential genes for the cellular and systemic homeostatic response to oxygen availability. To date, three HIF isoforms have been identified named HIF-1, HIF-2 and HIF-3. HIFs are composed by a constitutively expressed β and an oxygen-regulated α subunit.[11–13] In addition to the N-terminal and C-terminal transactivation domains, all HIFs contain an internal ODD domain (Oxygen-dependent Degradation Domain), which is necessary and sufficient for regulation of protein stability as a function of oxygen concentration.[14,15] The α subunits of HIFs are hydroxylated at prolines in normoxia (NMX) by oxygen-dependent active prolyl-4-hydroxylases.[16,17] Hydroxylated HIF-αs interact with the von Hippel–Lindau (VHL) gene product, the tumor suppressor pVHL, an essential component of the E3 ubiquitin ligase ECV (EloB/C-CUL2-pVHL) complex, which also includes Elongin B, Elongin C, Cullin-2 and Rbx-1.[18] Recognition of Prolil-hydroxyl-HIF-αs by pVHL is a prerequisite to allow the ECV complex to catalyze the polyubiquitination and subsequent degradation of α subunits by the 26S proteasome.[19,20] Prolyl-4-hydroxylases are not functional in HPX, pVHL binding is lost and consequently α subunits escape from normoxia-dependent degradation. Stable HIF-αs accumulate into the nucleus and associate with β subunits to induce genes involved in angiogenesis, erythropoiesis, cellular metabolism, invasion and metastasis, among others.[21] Discoveries in the recent years of new HIF regulatory pathways lead to the open question of the level of regulation that determines HIFs protein levels and action.[22]

Naturally occurring inactivating mutations of pVHL are associated with the VHL disease, a hereditary cancer syndrome characterized by development of hemangioblastomas of the central nervous system and retina, renal clear-cell carcinomas (RCCs) and pheochromocytoma.[23–25] As constitutive activation of HIFs has been linked with development and maintenance of a variety of high-vascularized solid human tumors, abnormal function of pVHL provides a permissive setting for the deregulation of HIF-1α and HIF-2α and therefore tumor formation.[13,25,26]

[1]Instituto de Investigación en Biomedicina de Buenos Aires (IBioBA)—CONICET—Partner Institute of the Max Planck Society, Buenos Aires, Argentina; [2]Departamento de Fisiología y Biología Molecular y Celular, Facultad de Ciencias Exactas y Naturales, Universidad de Buenos Aires, Buenos Aires, Argentina; [3]Center for Endocrinological Investigations (CEDIE), Hospital de Niños R. Gutiérrez, Buenos Aires, Argentina and [4]Department of Clinical Research, Max Planck Institute of Psychiatry, Munich, Germany. Correspondence: Dr E Arzt, Instituto de Investigacion en Biomedicina de Buenos Aires (IBioBA) -CONICET- Partner Institute of the Max Planck Society, Godoy Cruz 2390, Buenos Aires C1425FQD, Argentina.
E-mail: earzt@ibioba-mpsp-conicet.gov.ar
[5]These authors equally contributed to this work.
Received 29 May 2014; revised 22 October 2014; accepted 4 November 2014

pVHL mutations are classified in type 1, which are mostly deletions and truncations encoding inactive pVHL, and type 2, which are commonly missense mutations that lead to a partial pVHL loss of function.[27,28]

HIF-1α is sumoylated under HPX,[29] which is enhanced by RSUME.[1] Although sumoylation may contribute to stabilize HIF-1α,[29] it has been demonstrated that de-sumoylation stabilizes HIF-1α as well.[30] Therefore, the remaining question is whether other mechanisms involving RSUME have a role in HIFs stabilization.[22] The pattern of expression of RSUME in tumor necrotic areas and in tissues sensitive to VHL disease[1] led us to investigate the action of RSUME on pVHL. Thus, the aims of this study were to investigate: (a) the action of RSUME on pVHL-dependent HIFs-α stabilization, (b) the molecular mechanism by which RSUME acts on pVHL and stabilizes HIFs and (c) RSUME impact on pVHL-related tumor progression. In the present study, we demonstrate that RSUME action on pVHL is critical for pVHL function in normal and pathological stages.

RESULTS

RSUME stabilizes HIF by targeting pVHL

We determined that RSUME increases HIF-1α protein levels in the presence of pVHL (Figure 1a lane 4 vs 3). RSUME has a similar action (Figure 1a lanes 2 and 4) as the proteasomal degradation blockage with the inhibitor MG-132 (Figure 1a lanes 5 and 7). Incubation with MG-132 in the presence of RSUME results in slightly elevated levels of HIF-1α (Figure 1a lanes 6 and 8 vs 5 and 7, respectively). In order to recapitulate HIF-1α degradation/stabilization transition, cells were transiently transfected with pVHL and/or RSUME expression vectors and then incubated at NMX or at 3.5 or 7 h of HPX. pVHL overexpression leads to a decrease in HIF-1α protein levels at all times of HPX assayed (Figure 1b lanes 8–9 vs 2–3), and RSUME increases HIF-1α protein stability in spite of pVHL overexpression in normoxic and hypoxic cells (Figure 1b lanes 4–6 vs 1–3 and 10–12 vs 7–9).

RSUME increases the stability of a constitutively expressed ODD-LUC reporter gene (Figure 1c bars 2 vs 1). Interestingly, RSUME has no effect on HIF-α stability in pVHL-defective cells (Figure 1c bars 4 vs 3), unless ectopic pVHL is expressed (Figure 1c bars 6 vs 5). RSUME also counteracts pVHL when a reporter gene for HIF transcriptional activity was used (Supplementary Figure 1).

Taken together, these results indicate that RSUME inhibits pVHL action on HIF and thus increases HIF protein stability by inhibiting pVHL function.

RSUME interaction with pVHL

To explore the molecular basis by which RSUME inhibits pVHL, we addressed whether RSUME would act modifying pVHL interactions. We found that increasing amounts of overexpressed RSUME decreases the levels of HIF-1α associated to pVHL (Figure 2a lanes 6–10). RSUME interacts with pVHL (Figure 2a lanes 7–10), and this interaction seems to be HIF-1α independent (Figure 2b). Indeed, RSUME also interacts with pVHL in HPX (Supplementary Figure 2).

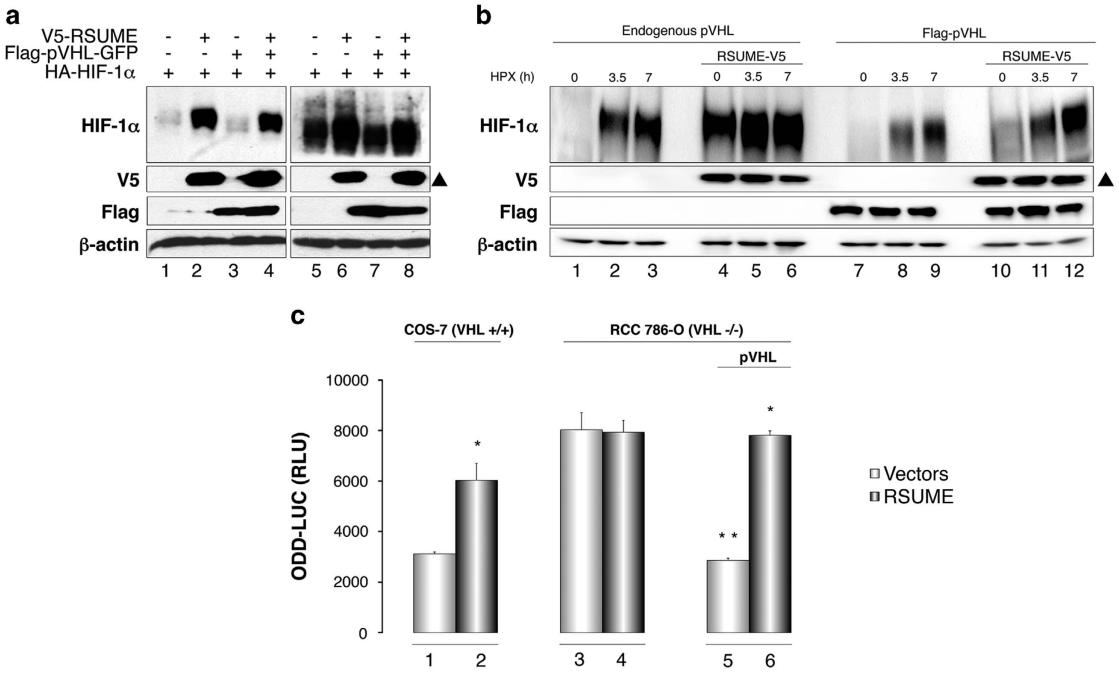

Figure 1. RSUME action takes place upstream of HIF. (**a**) COS-7 cells were transfected with 0.5 μg of V5-RSUME and/or 0.5 μg of Flag-pVHL-GFP and 0.5 μg of HA-HIF-1α expression vectors. 48 h post transfection, cells were incubated in 2% serum 5 μM MG-132 (Lanes 5-8) or vehicle for 6 h (Lanes 1-4). Cells were lysed and the extracts were subjected to SDS–polyacrylamide gel electrophoresis (SDS–PAGE) and WB using the indicated antibodies. β-Actin was used as loading control. One representative experiment from three independent experiments with similar results is shown. ▲RSUME. (**b**) COS-7 cells were transfected with 0.5 μg of HA-HIF-1α and/or 0.5 μg of RSUME and/or 0.5 μg of Flag-pVHL-GFP expression vectors. 48 h post transfection, cells were incubated under normoxia (NMX; 37 °C, 21% O_2, 5% CO_2) or hypoxia (HPX; 37 °C, 1% O_2, 5% CO_2) for 3.5 or 7 h. Cells were lysed and the extracts were subjected to SDS–PAGE and WB using the indicated antibodies. β-Actin was used as loading control. Similar results were obtained at 2 and 5 h of HPX. One representative experiment from three independent experiments with similar results is shown. ▲RSUME. (**c**) COS-7 and RCC-786-O cells were transfected with 0.7 μg of ODD-LUC reporter vector, 0.3 μg of pRK5-Gaussia-LUC control vector and/or 0.5 μg of RSUME and/or 0.5 μg of Flag-pVHL-GFP expression vectors. 24 h post transfection *Firefly* luciferase (LUC) was measured. Each value was normalized by *Gaussia* LUC activity. Results are expressed as mean ± s.e.m. of triplicates of one representative experiment of three experiments with similar results. *$P < 0.05$ compared with cells with the corresponding empty vector (bar 1 in COS-7 and bar 5 in RCC-786-O). **$P < 0.05$ compared with RCC-786-O cells transfected with empty vectors (bar 3). Analysis of variance with Scheffé's test.

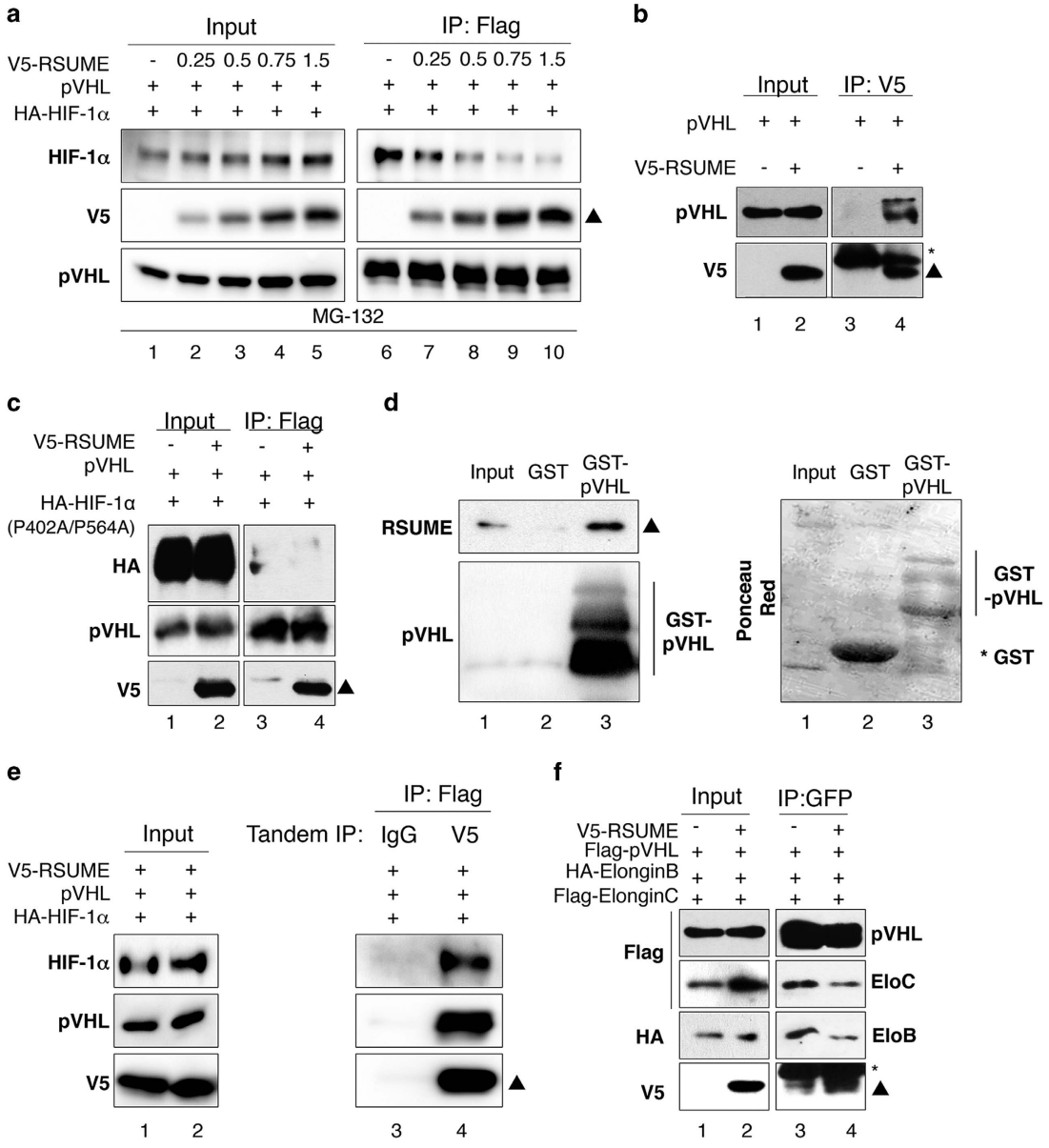

Figure 2. RSUME interacts with pVHL, inhibits pVHL/HIF-1α interaction and affects the ECV complex assembly. (**a**) COS-7 cells were transfected with 0.5 μg of HA-HIF-1α, 0.5 μg of pVHL (Flag-pVHL-GFP) and/or increasing amounts of V5-RSUME (0.25, 0.5, 0.75 and 1.5 μg) expression vectors. 48 h post transfection, cells were incubated in 2% serum, 5 μM MG-132 for 6 h. Cells were lysed and immunoprecipitated with anti-FLAG antibodies. Immunoprecipitated fractions and lysate aliquots (Input) were subjected to SDS–polyacrylamide gel electrophoresis (SDS–PAGE) and WB using the indicated antibodies. One representative experiment from two independent experiments with similar results is shown. ▲RSUME. (**b**) COS-7 cells were transfected with 0.5 μg of pVHL (Flag-pVHL-GFP) and/or 0.5 μg of V5-RSUME expression vectors. Cells were lysed and immunoprecipitated with anti-V5 antibodies. Immunoprecipitated fractions and lysate aliquots (Input) were subjected to SDS–PAGE and WB using the indicated antibodies. One representative experiment from two independent experiments with similar results is shown. *Immunoglobulin light chain; ▲RSUME. (**c**) COS-7 cells were transfected with 0.5 μg of pVHL (Flag-pVHL-GFP), 0.5 μg of HA-HIF-1αP402A/P564A and/or 0.5 μg of V5-RSUME expression vectors. 48 h post transfection, cells were lysed and immunoprecipitated with anti-FLAG antibodies. Immunoprecipitated fractions and lysate aliquots (Input) were subjected to SDS–PAGE and WB using the indicated antibodies. One representative experiment from two independent experiments with similar results is shown. ▲RSUME. (**d**) 7.5 μg of recombinant RSUME was co-precipitated with 2.5 μg of GST-pVHL *in vitro*. Pulled-down fractions and input were subjected to SDS–PAGE and WB using the indicated antibodies. As internal control, to detect unspecific binding, GST alone was used to pull down RSUME. As pull-down control, Ponceau red staining of the blot shows both GST and GST-VHL purification (right panel). One representative experiment from two independent experiments with similar results is shown. ▲RSUME. (**e**) COS-7 cells were transfected with 0.5 μg of HA-HIF-1α, 0.5 μg of pVHL (Flag-pVHL-GFP) and 0.5 μg of V5-RSUME expression vectors. 48 h post transfection, cells were incubated in 2% serum 5 μM MG-132 for 6 h. Cells were lysed and a first immunoprecipitation (IP) using anti-FLAG antibodies was performed. Immunoprecipitated fractions were eluted with soluble FLAG peptide and a second IP using anti-V5 antibodies was performed. Immunoprecipitated fractions from second IP (Tandem IP) and lysate aliquots (input) were subjected to SDS–PAGE and WB using the indicated antibodies. One representative experiment from two independent experiments with similar results is shown. ▲RSUME. (**f**) COS-7 cells were transfected with 0.5 μg of pVHL (Flag-pVHL-GFP), 0.5 μg of Flag-Elongin C, 0.5 μg of HA-Elongin B, 0.5 μg of Cullin-2 and/or 0.5 μg of V5-RSUME expression vectors. 48 h post transfection, cells were lysed and immunoprecipitated with the indicated antibodies. Immunoprecipitated fractions and lysate aliquots (input) were subjected to SDS–PAGE and WB using the indicated antibodies. One representative experiment from two independent experiments with similar results is shown. *Immunoglobulin light chain; ▲RSUME.

To verify if the pVHL/RSUME interaction is HIF-1α independent, we first used a HIF-1α mutant (HIF-1αP402A/P564A) unable to be hydroxylated at Prolines 402 and 564 and to bind pVHL.[31] pVHL/RSUME interaction occurs in the absence of pVHL/HIF-1α interaction (Figure 2c lane 4 vs 3). In addition, to unequivocally prove the direct interaction of RSUME with pVHL (in the absence of HIFs), we performed an *in vitro* pull-down experiment in which the direct physical interaction of RSUME and pVHL is observed (Figure 2d). Moreover, by performing tandem immunoprecipitation (first purification: pVHL-associated proteins; second purification: RSUME-associated proteins), we demonstrate that RSUME/pVHL/HIF-1a coexist in the same protein complex (Figure 2e lane 4). As pVHL binds Elongin C, Elongin B and Cullin-2 to form active E3 ligase, we also studied RSUME action on ECV complex assembly. RSUME inhibits pVHL binding to Elongin C and Elongin B (Figure 2f lane 4 vs 3).

RSUME inhibits pVHL-dependent HIF-1α ubiquitination

To determine whether RSUME affects substrate ubiquitination, we performed *in vitro* ubiquitination assays of recombinant GST or GST-ODD (previously *in vitro* hydroxylated to allow pVHL binding) using cell extracts of transfected COS-7 cells as a source of enzymatic E1, E2 and E3 activities. Impaired ubiquitination of GST-ODD is evident when cell extracts containing RSUME are used as a source of enzymatic activity (Figure 3a lane 2 vs 1), indicating that RSUME inhibits HIF-1α ubiquitination. Although pVHL overexpression increases HIF-1α ubiquitination (Figure 3b, lane 7 vs 5), RSUME inhibits both basal and pVHL-induced HIF-1α ubiquitination (Figure 3b, lanes 6 vs 5 and 8 vs 7, respectively). Affinity purification of ubiquitinated proteins confirmed that RSUME inhibits basal and pVHL-induced HIF-1α ubiquitination (Supplementary Figure 3). Silencing endogenous RSUME increases the amount of ubiquitinated HIF-1α associated to pVHL (Figure 3c lanes 5 vs 1 and 3). Moreover, it also increases the interaction between pVHL and HIF-1α (Figure 3c, western blot (WB): HIF-1α lanes 5 vs 1 and 3). These effects also take place after silencing overexpressed RSUME (Figure 3c lane 6 vs 4 and 2).

RSUME increases pVHL sumoylation

Considering that RSUME is an enhancer of sumoylation, we analyzed the contribution of this activity on pVHL. Affinity purification of sumoylated proteins from transiently transfected cells expressing His-SUMO-2 shows increased SUMO conjugation to pVHL when RSUME is overexpressed (Figure 4a lanes 9 vs 8). Co-transfection of RSUME with the pVHL E3 SUMO ligase PIASy[32] does not increase pVHL sumoylation (Figure 4a lanes 11 vs 10). Similar results were obtained in cell lysates in the presence of SUMO and RSUME (Supplementary Figure 4a). *In vitro* sumoylation assays show that RSUME enhances SUMO-1 conjugation to GST-VHL (Figure 4b lanes 5 vs 4). pVHL sumoylation is inhibited by silencing endogenous RSUME (Figure 4c lanes 7 vs 6). A non-sumoylable pVHL variant (pVHLK171R)[32] was used in the *in vitro* and *in vivo* sumoylation assays to confirm the identity of bands corresponding to SUMO-conjugated pVHL (Figures 4b and c). The increase in pVHL SUMO conjugation by RSUME occurs both in normoxia and in HPX (Supplementary Figure 4b). In agreement with the fact that pVHL sumoylation inhibits HIF-1α degradation,[32,33] SUMO increases ODD-LUC protein stability, and reverts the pVHL-induced inhibition (Figure 4d bar 2 vs 1, and bar 5 vs 4). Consistent with its action on pVHL sumoylation, RSUME acts similarly as SUMO (Figure 4d bar 3 vs 1 and 2 vs 6 and 4 and 5).

RSUME is expressed in human pVHL-deficient tumors and is critical for the pVHL mutant phenotype

RSUME is expressed in human pheochromocytoma and hemangioblastoma and in RCC-786-O cell line (Figures 5a and b), which contain high levels of HIF-2α, but not the other isoforms of HIF-α. Interestingly, in these pVHL-deficient cells, RSUME action on endogenous HIF-2α stability is only detected when pVHL is ectopically expressed (Figure 5c lanes 4 vs 3). Similar to what observed with HIF-1α, we found that RSUME inhibits pVHL/HIF-2α interaction (Figure 5d lanes 4 vs 3) and that RSUME acts inhibiting HIF-2α ubiquitination (Figure 5e lanes 8 vs 7). We have previously shown that RSUME mRNA expression is induced by HPX, which, as is shown now, occurs at early stages of HPX (Supplementary

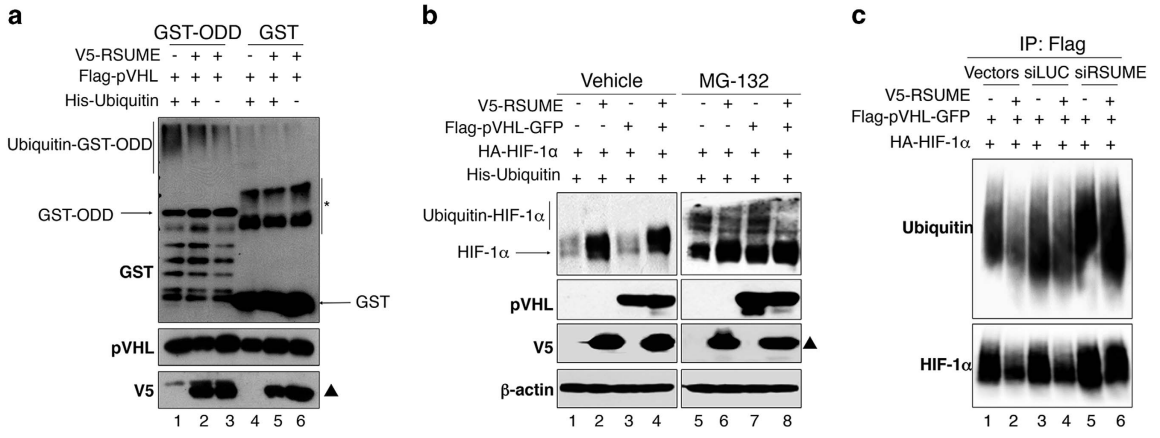

Figure 3. RSUME inhibits pVHL-dependent HIF-1α ubiquitination. (**a**) 1.0 μg of *in vitro* hydroxylated recombinant GST-ODD or GST were incubated at 30 °C for 1 h with cell extracts of COS-7 cells previously transfected with 0.5 μg of Flag-pVHL, 0.5 μg of HA-Elongin B, 0.5 μg of Flag-Elongin C, 0.5 μg of HA-Cullin-2 and/or V5-RSUME and/or His-Ubiquitin expression vectors. Reaction mixes were subjected to SDS–polyacrylamide gel electrophoresis (SDS–PAGE) and WB using the indicated antibodies. One representative experiment from three independent experiments with similar results is shown. *Uncharacterized GST immunoreactive band; ▲RSUME. (**b**) COS-7 cells were transfected with 0.5 μg of HA-HIF-1α, 0.5 μg of His-Ubiquitin, and/or 0.5 μg of V5-RSUME and/or 0.5 μg of Flag-pVHL expression vectors. 48 h post transfection, cells were incubated in 2% serum 5 μM MG-132 or vehicle for 6 h. Cells were lysed and cell extracts were subjected to SDS–PAGE and WB using the indicated antibodies. β-Actin was used as loading control. One representative experiment from four independent experiments with similar results is shown. ▲RSUME. (**c**) COS-7 cells were transfected with 0.5 μg of HA-HIF-1α, 0.5 μg of Flag-pVHL and/or 0.5 μg of V5-RSUME and/or siLUC and/or siRSUME expression vectors. 48 h post transfection, cells were lysed and immunoprecipitated with the FLAG antibody. Immunoprecipitated fractions and lysate aliquots (Input) were subjected to SDS–PAGE and WB using the indicated antibodies. One representative experiment from two independent experiments with similar results is shown.

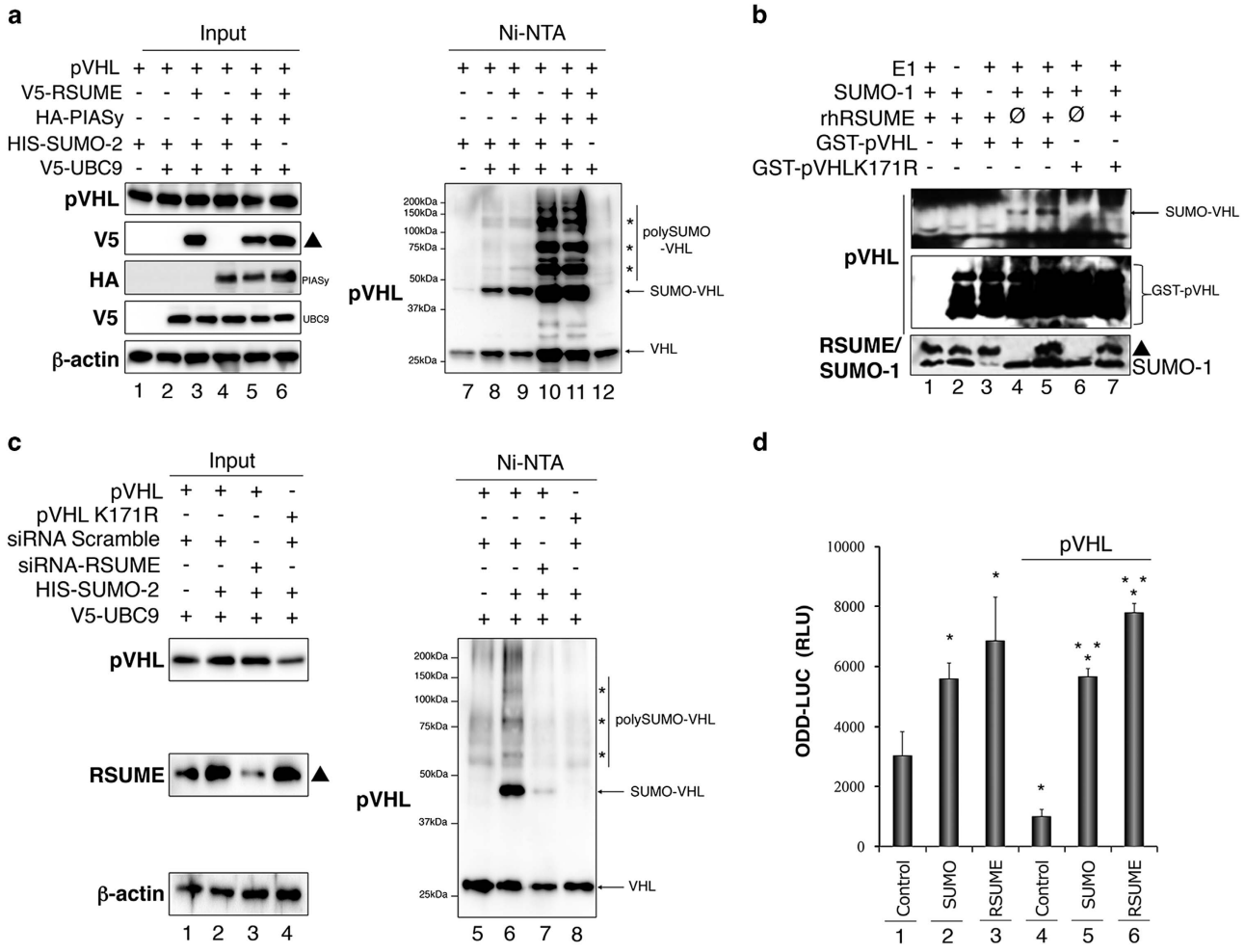

Figure 4. RSUME enhances pVHL sumoylation. (**a**) COS-7 cells were transfected with 0.6 μg of Flag-pVHL and/or 0.6 μg 6xHis-SUMO-2 and/or 0.1 μg of V5-Ubc9 and/or 0.05 μg of V5-RSUME and/or 0.1 μg of HA-PIASy expression vectors. 48 h post transfection, cells were harvested, an aliquot of the lysates was directly analyzed by WB (Input) and the remaining extracts were used for Ni^{2+} affinity chromatography to purify 6xHis-SUMO-2 (Ni-NTA). Purified fraction and Inputs were subjected to SDS–polyacrylamide gel electrophoresis (SDS–PAGE) and WB using the indicated antibodies. One representative experiment from two independent experiments with similar results is shown. β-Actin was used as a loading control (input). ▲RSUME. (**b**) *In vitro* SUMO-1 conjugation of recombinant GST-pVHL and GST-pVHLK171R assayed in the presence or absence of 0.5 μg of recombinant human RSUME protein (rhRSUME). Reaction mixes were subjected to SDS–PAGE and WB using the indicated antibodies. One representative experiment from two independent experiments with similar results is shown. ∅: control protein extract purified from *E. coli* transformed with the empty pQE30 vector. ▲RSUME. (**c**) COS-7 cells were transfected with 20 μM siRNA against RSUME or Scramble as a control, 0.6 μg of Flag-pVHL or Flag-pVHLK171R, 0.1 μg of V5-Ubc9 and/or 0.6 μg 6xHis-SUMO-2 expression vectors. 48 h post transfection, cells were harvested, an aliquot of the lysates was directly analyzed by WB (Input) and the remaining extracts were used for Ni^{2+} affinity chromatography to purify 6xHis-SUMO-2 (Ni-NTA). Purified fraction and Inputs were subjected to SDS–PAGE and WB using the indicated antibodies. One representative experiment from two independent experiments with similar results is shown. β-Actin was used as a loading control (input). ▲RSUME. (**d**) COS-7 cells were transfected with 0.7 μg of ODD-LUC reporter vector, 0.3 μg of pRK5-Gaussia-LUC control vector and/or 0.5 μg of RSUME, and/or 0.5 μg of Flag-pVHL and/or 0.3 μg of HA-SUMO-1 expression vectors. After 24 h, cells were harvested and *firefly* luciferase (LUC) was measured. Each value was normalized by *Gaussia* LUC activity. Results are expressed as mean ± s.e.m. of triplicates of one representative experiment of three experiments with similar results. $*P < 0.05$ compared with cells transfected with the empty vector (bar 1). $**P < 0.05$ compared with cell transfected with pVHL (bar 4). Analysis of variance with Scheffé's test.

Figure 5). As depicted in Figures 5f and g, wild-type pVHL inhibits RSUME expression at transcriptional level, constituting a feedback loop. Interestingly, the ability of wild-type pVHL to inhibit RSUME transcription is completely lost in pVHL type 2 mutants (Figure 5g, bars 3–5 vs bar 2).

As several pVHL mutants show impaired HIF-α regulation, we investigated the ability of RSUME to modulate the function of these type 2 pVHL mutants. We analyzed cells negative for pVHL transfected with the components of the machinery under study: pVHL WT or mutated, RSUME overexpression or its silencing, and the HIF-1α ODD-LUC as reporter of the action of pVHL. We used Tyr112His, Arg167Gln and Leu188Val as representative of type 2A, type 2B and type 2C pVHL mutants, respectively.[34] Consistent with previous reports on HIF-1α and HIF-2α,[34–36] all type 2 pVHL mutants on their own are partially active in driving HIF (ODD-LUC in our experiment) downregulation in normoxia (Figure 5h bars 5, 7 and 9 vs 1). RSUME co-expression produces complete loss of pVHL function of these mutants activity resulting in increased ODD stability (Figure 5h bars 6, 8 and 10 vs 5, 7 and 9, respectively). By silencing endogenous RSUME, pVHL activity of all Type 2 pVHL mutants becomes potent (Figure 5i bars 6, 8 and 10 vs 5, 7 and 9, respectively) and similar to wild-type pVHL (Figure 5i bars 6, 8 and 10 vs bar 4), indicating that RSUME is necessary for the functional impact of pVHL mutations.

In order to elucidate in an *in vivo* tumor model the contribution of the direct regulation of pVHL function by RSUME, we evaluated tumor formation and vascularization in a pVHL model devoid of HIF-1α that depends on HIF-2α. Visible tumors developed between 50 and 90 days in mice injected either with RCC-786-O cells or in clones stable transfected with a Scramble short haripin RNA together with either wild-type pVHL or Leu188Val pVHL (Figure 6a). Those clones in which the co-transfection of pVHL

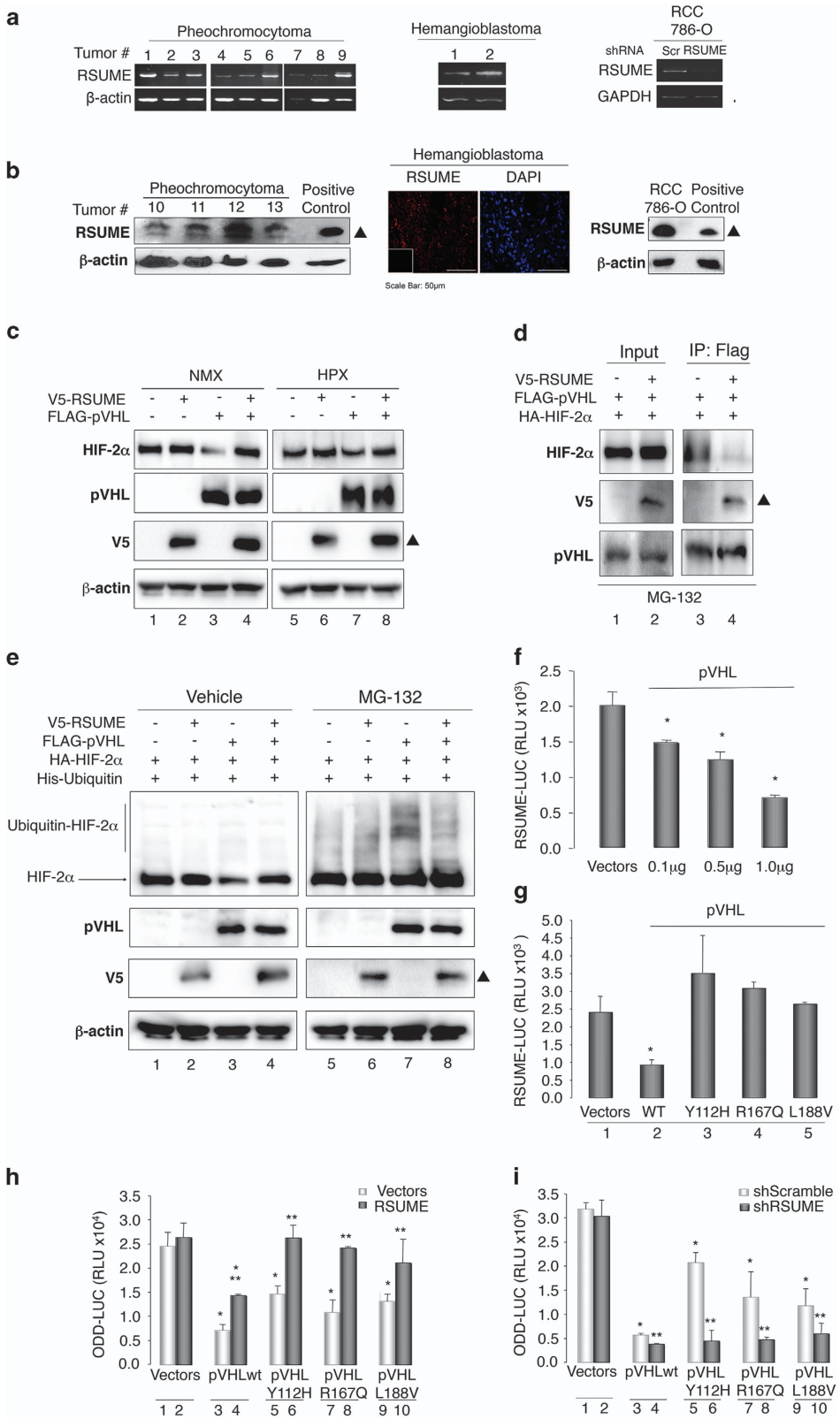

variants was performed with a shRSUME to specifically silence endogenous RSUME (Supplementary Figure 6), showed a significant reduction of the tumor size (Figure 6a and quantified in Figure 6d). These results support the notion of a pVHL stronger activity in the absence of RSUME. Moreover, consistent with the results on HIF activity, pVHL Leu188Val, loses its mutant phenotype in clones in which RSUME is silenced, showing a functional pVHL action. Consistent with this, HIF-2α and vascular endothelial growth factor A (VEGF-A) levels are significantly reduced in tumors in the absence of RSUME (Figure 6b, Supplementary Figure 7 and quantified in Figure 6e). Moreover, vessel density is diminished when RSUME is silenced, compared with tumors derived from RCC-786-O cells without any treatment or in clones stably transfected with a Scramble short haripin RNA (Figure 6c and quantified in Figure 6f). Interestingly to note, the action of RSUME knockdown is more pronounced on VEGF-A and vascularization than on proliferation, consistent with the described role of HIF-2α.[37]

DISCUSSION

We demonstrate the critical role and describe the molecular mechanisms of RSUME action on pVHL-dependent HIF degradation (summarized in Figure 7). RSUME acts inhibiting pVHL function on the ODD domain: it increases pVHL sumoylation, interacts with pVHL in a HIF-1α-independent manner, inhibits the ECV complex assembly, and consequently pVHL-induced HIF-1/2α ubiquitination and degradation. RSUME does not act on HIF in pVHL-deficient cells, is expressed in VHL disease-related tumors and is instrumental for the loss of function of type 2 pVHL mutants. Moreover, RSUME knockdown impairs HIF-2-mediated tumor formation and vascularization in xenografts of both pVHL WT and a model of VHL disease.

It has been described that HIF-1 and 2α are substrates of sumoylation.[1,29,30,38,39] SUMO expression and conjugation to several proteins, including HIF-1α and pVHL, is stimulated by HPX and ischemia.[32,33,40,41] Particularly, HIF-1α sumoylation is finely modulated. HIF-1α is sumoylated under HPX,[29] which is enhanced by RSUME[1] and PIASγ;[38] and de-sumoylated by SENP1[30] and SENP3,[42] which acts on the coactivator of HIF-1α, p300, rather than on HIF-1α itself.[42] All these actions contribute to determine HIF-1α protein levels and transactivation.[22] It has been shown that short haripin RNA against RSUME (although its efficiency was not tested) did not lead to a change in the level of SUMO-modified HIF-2α in hypoxic conditions.[39] In addition to pVHL-independent RSUME stimulation of SUMO conjugation to HIF-1α during HPX,[1] indirect action of RSUME in the *in vitro* ubiquitination assay indicates that RSUME acts regardless of HIF-1α sumoylation status. In fact, we demonstrate that RSUME also stabilizes HIFs-α under normoxic conditions (active pVHL), inhibiting pVHL-dependent ubiquitination. In this line, the experiment silencing RSUME on pVHL$^{-/-}$ (reconstituted with either WT or mutated VHL), HIF-1α^{-}/HIF-2α^{+}cells, highlights the critical contribution of the action of RSUME directly on pVHL during normoxia. Interestingly, RSUME is expressed in normoxia and is rapidly induced in HPX, a kinetic that might reflect the role of RSUME in HIF degradation/stabilization during normoxia–hypoxia transition.

RSUME is expressed differentially in cells with high tumoral and angiogenic potential[1,5,43] and has been associated with the gene expression signature of breast cancer patients.[6,7] Using expression vectors of representative type 2 pVHL mutants, we show that all the mutants assayed lack the ability to negatively regulate RSUME expression. In accordance with this, we found high RSUME mRNA and protein levels in tumoral human pheochromocytoma and hemangioblastoma, and in the tumoral pVHL/HIF-1-defective cell line RCC-786-O. Interestingly, a bioinformatics analysis[44,45] of data from a clear cell renal cell carcinoma study from the Cancer Genome Atlas Research Network [46] shows that 4% of RCC tumors present high levels of RSUME mRNA and that these patients present decreased survival.

There is a genotype–phenotype correlation between naturally occurring type 2 mutations of pVHL in humans; type 2A mutations show high predisposition to pheochromocytoma and hemangioblastoma; type 2B show high risk to pheochromocytoma,

Figure 5. *RSUME* is expressed in VHL-related tumors and participates in the loss of function phenotype of type 2 pVHL mutants. (**a**) RT–PCR performed to detect endogenous RSUME expression in different human pheochromocytoma and hemangioblastoma tumor samples. β-Actin was used as a loading control (left and middle panels). RCC-786-O cells were transfected with 0.5 μg of shRSUME or shScramble (control) expression vector and 48 h post transfection, cells were lysed for RT–PCR assays to detect RSUME expression, GAPDH was used as loading control (right panel). (**b**) WB performed to detect endogenous RSUME expression in different human pheochromocytoma tumor samples. β-Actin was used as a loading control (left panel). Immunofluorescence performed to detect endogenous RSUME (red; 1:200) in a fixed human hemangioblastoma. Nuclei were stained with 4′,6-diamidino-2-phenylindole (DAPI; blue).The corresponding negative control, omitting primary antibody, is inserted at the left corner of anti-RSUME picture (middle panel). WB performed to detect endogenous RSUME expression in RCC-786-O cell line. β-Actin was used as a loading control (right panel). For WB, COS-7 cell extract of cells transfected with V5-RSUME were used as positive control. ▲RSUME. (**c**) RCC-786-O cells were transfected with 0.5 μg of V5-RSUME and/or 0.5 μg Flag-pVHL-GFP. 48 h post transfection, cells were incubated under normoxia (NMX) (Lanes 1-4) or hypoxia (HPX) (Lanes 5-8) for 16 h. Cells were lysed and the extracts were subjected to SDS–polyacrylamide gel electrophoresis (SDS–PAGE) and WB using the indicated antibodies. β-Actin was used as loading control. One representative experiment from three independent experiments with similar results is shown. ▲RSUME. (**d**) RCC-786-O cells were transfected with 0.5 μg of pVHL (Flag-pVHL-GFP), and/or 0.5 μg of V5-RSUME and 0.5μg HA-HIF-2α expression vectors. 48 h post transfection, cells were incubated in 2% serum 5 μM MG-132 for 6 h. Cells were lysed and immunoprecipitated with the indicated antibodies. Immunoprecipitated fractions and lysate aliquots (Input) were subjected to SDS–PAGE and WB using the indicated antibodies. One representative experiment from two independent experiments with similar results is shown. ▲RSUME. (**e**) RCC-786-O cells were transfected with 0.5 μg of HA-HIF-2α, 0.5 μg of His-Ubiquitin, and/or 0.5 μg of V5-RSUME and/or 0.5 μg of Flag-pVHL expression vectors. 48 h post transfection, cells were incubated with 5 μM MG-132 or vehicle for 6 h. Cells were lysed and cell extracts were subjected to SDS–PAGE and WB using the indicated antibodies. β-Actin was used as loading control. One representative experiment from three independent experiments with similar results is shown. ▲RSUME. (**f** and **g**) RCC-786-O (**f**) and A498 (**g**) cells were transfected with 0.7 μg of RSUME-LUC reporter vector, 0.3 μg of pRK5-Gaussia-luciferase (LUC) control vector and 0.1, 0.5 or 1.0 μg of Flag-pVHL (**f**) or 0.5 μg of HA-pVHL or each HA-pVHL mutant (Y112H, R167Q, L188V) (**g**) expression vectors. 24 h post transfection, cells were harvested and *Firefly* LUC was measured. Each value was normalized by *Gaussia* LUC activity. Results are expressed as mean ± s.e.m. of triplicates of one representative experiment of three experiments with similar results. $^{*}P < 0.05$ compared with cells transfected with the empty vector (analysis of variance (ANOVA) with Scheffé's test). (**h** and **i**) RCC-786-O cells were transfected with 0.7 μg of ODD-LUC reporter vector, 0.3 μg of pRK5-Gaussia-LUC control vector, 0.5 μg of HA-pVHL or 0.5 μg of each HA-pVHL mutant (Y112H, R167Q, L188V) and/or 0.5 μg of V5-RSUME (**h**) or 0.5 μg of shRSUME or shScramble (control) (**i**) expression vectors. 24 h post transfection, cells were harvested and *Firefly* LUC was measured. Each value was normalized by *Gaussia* LUC activity. Results are expressed as mean ± s.e.m. of triplicates of one representative experiment of three experiments with similar results. $^{*}P < 0.05$ compared with cells transfected with the empty vector (bar 1). $^{**}P < 0.05$ compared with cells with the corresponding empty vector (**h**) or Scramble (**i**) (ANOVA with Scheffé's test).

hemangioblastoma and renal cell carcinoma, and type 2C show high risk to pheochromocytoma.[23] It has been proposed that the differences in tumor risk are consequences of different abilities to ubiquitinate HIF-1α by each pVHL mutant subtypes.[47,48] The impact of missense mutations on the function of pVHL seems to be highly diversified ranging from imperceptible to complete

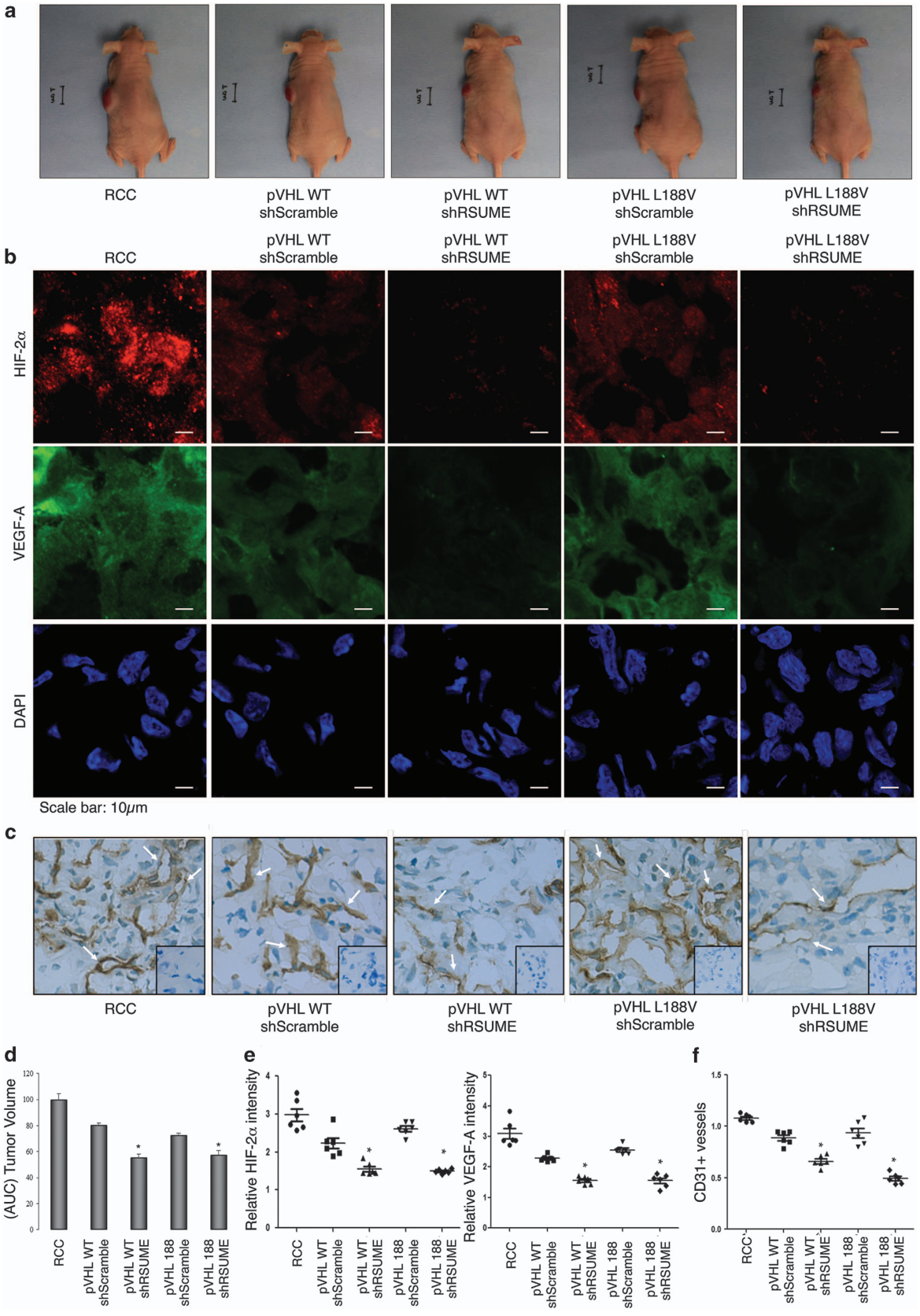

functional loss, with similar patterns observed for HIF-1α and HIF-2α.[34–36,49] Defects on HIF-1α regulation by type 2C pVHL mutants have been reported.[50] Slightly elevated HIF-1α levels are detectable in pVHL-defective cell clones expressing type 2C pVHL mutants.[47] VHL mutations linked to type 2C VHL disease have also shown to preserve the ability to negatively regulate HIF-1α and HIF-2α.[47] All this evidence suggests that the ability to negatively regulate HIF-1/2α by each pVHL mutant subtype depends at least on other (co-)factors. In this work, using transiently transfected RCC-786-0 cells, we recapitulate the phenotype of different types of representative mutants of type 2 mutation subtype (type 2A pVHL Y112H, type 2B pVHL R167Q and type 2C pVHL L188V) showing partial ODD-LUC reporter regulation. Interestingly, complete loss of function of all three types of pVHL type 2 mutants only occurs when RSUME is co-expressed. Moreover, we show that RSUME silencing restores wild-type pVHL function of these mutants, which have pVHL action in complete absence of RSUME. Taken together, these results indicate a strong negative correlation between RSUME levels and pVHL function and might be related to the cell/tissue type-specific tumorigenicity of pVHL mutations. The fact that pVHL mutants also restore normoxia regulation of HIF-1α or have different results in different systems may be explained by the co-expression levels of RSUME.

In clear-cell renal carcinoma, an important disease and the most common form of kidney cancer, the pVHL tumor suppressor is often inactivated, leading to constitutive expression and action of HIF-1α, HIF-2α or both. As stated in a recent update on the pathology, beside the relevance of the mutations, RCC pathophysiology may hinge more on the end effect of pVHL inactivation and consequent degradation of HIF-1 and/or 2α.[51] In RCC cells, we show that RSUME presence is involved in the manifestation of pVHL mutant phenotype. As highlighted recently, discovery of new markers is of great importance in RCC.[52,53]

To confirm *in vivo* the RSUME involvement in pVHL function, we used pVHL-deficient cells to generate clones stably expressing wild-type or type 2C pVHL mutant, in which we show that silencing endogenous RSUME inhibits the tumorigenicity of these cells when injected in nude mice. Confirming the mechanistic data, HIF-2α, its regulated angiogenic factor VEGF-A and the marker of vessels formation (CD31) are inhibited in the clones expressing the shRSUME. Accordingly, it has been shown that VHL reintroduction[54,55] or HIF inhibition[56] in pVHL-deficient RCC cells is sufficient to suppress tumor growth in nude mice xenograft assays. Normoxic stabilization of HIF-1α was not sufficient to reproduce tumorigenesis in pVHL-reconstituted RCC cells,[57] indicating that other mechanisms or players are involved. According to our results, RSUME co-expression is instrumental for pVHL lack of action on the HIF ODD domain, impacting on its downstream targets. In accordance with the results in cell culture, RSUME contributes to confer its phenotype to pVHL mutants when *in vivo* tumorigenicity is examined, confirming that RSUME has an essential role in the impact of VHL mutations. The ability of RSUME to modulate wild-type and type 2 mutant phenotype of VHL, in conjunction with the expression of RSUME in pVHL-related tumors, highlights a central role of RSUME in ECV homeostasis and its impact in VHL disease tumorigenesis.

MATERIALS AND METHODS

Materials

Unless otherwise stated, reagents were obtained from Life Technologies or Sigma Chemical Co.

Plasmids and cloning

The following plasmids were kindly provided and cited by: HIF-1α, Lee;[58] pCEFL, Coso;[59] Flag-pcDNA3-GFP and Flag-pVHL-GFP, Lee;[60] ODD-LUC, pcDNA3-LUC,[61] HA-HIF-1αP402A/P564A[31] and HA-HIF-2α,[62] Kaelin; pBI-GLV4R HRE-LUC, Van Meir;[63] Gaussia-KDEL, Schülke; Flag-pVHL, Flag-Elongin C, HA-Elongin B and HA-Cullin2, Schoenfeld;[64] His-Ubiquitin, Trecier; HA-SUMO-1, HA-SUMO-2, V5-Ubc9 and 6xHis-SUMO-2, Hay;[65–67] Flag-pVHL; STII, STII-HA-pVHL,STII-HA-pVHL Y112H, R167Q and L188V, Rathmell;[34] siRSUME and siScramble;[1] shRSUME and shScramble (Insert sequences: 5′-GGAGAAGTGGGCTTCAGATTT-3′ and 5′-GGAATCTCATTCGA TGCATAC-3′ for shRSUME and shScramble, respectively, #KH14185N, SABiosciences, Hilden, Germany); GST-ODD, V5-RSUME, His-RSUME and RSUME-LUC were obtained as described.[1] The nucleotide sequences of all constructs were confirmed by DNA sequencing.

Cell culture

COS-7 cells were obtained from American Type Culture Collection (Manassas, VA, USA), RCC 786-O cells were obtained from R Voest, University Medical Center Utrecht, and A498 cells from R Blaheta, Johann

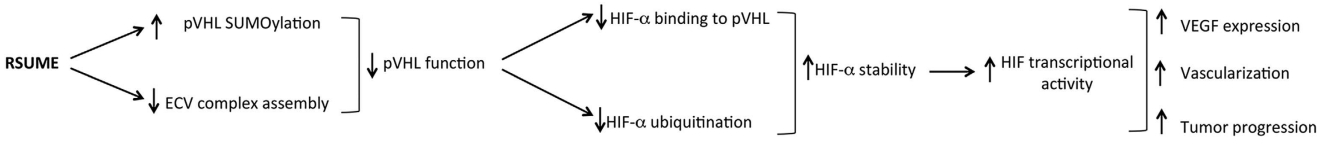

Figure 7. RSUME actions on pVHL-HIFs-α. RSUME main actions on pVHL-HIFs-alpha are outlined. RSUME sumoylates pVHL and negatively regulates the assembly of the complex between pVHL, Elongins and Cullins (ECV), inhibiting HIF-1 and 2α ubiquitination and degradation. Increased HIF-1 and 2α transcriptional activity may trigger VEGF expression, vascularization and tumor progression.

Figure 6. RSUME is involved in pVHL loss-of-function-dependent tumor formation. (**a**) RCC-786-O clone cells were injected subcutaneously in to male athymic nude mice (5×10^6 cells, each clone). Photographs shown were taken at 70 days after injection. One mouse with similar results to the others of each group is shown. Two independent experiments with four mice in each group in each experiment were performed, showing similar results. (**b**) Tumor cryosections were stained by triple immunofluorescence with the indicated antibodies: HIF-2α (red; 1:100), VEGF-A (green; 1:100) and 4′,6-diamidino-2-phenylindole (DAPI) for staining cell nuclei (blue). Images were acquired with at ×60 magnification. One representative picture for each clone is shown. (**c**) To visualize tumor vascularization, tumor cryosections were immunostained by immunohistochemistry for the endothelial cell marker CD31 (1:500). Images were acquired at ×40 magnification. The corresponding negative controls, omitting primary antibody are inserted at the right corner of each picture. One representative picture for each clone is shown. Arrows indicate CD31+ (brown) endothelial cells. (**d**) Area under the curve (AUC) calculation for tumor volume is shown. Results are shown as mean ± s.e.m. $^*P < 0.05$ compared with the corresponding Scramble clone (analysis of variance (ANOVA) with Scheffé's test). Two independent experiments with four mice in each group in each experiment were performed, showing similar results. (**e**) HIF-2α and VEGF-A were quantified and relativized to DAPI signal. Results obtained from six independent pictures for each condition are expressed as mean ± s.e.m. $^*P < 0.05$ compared with the corresponding Scramble clone (ANOVA with Scheffé's test). (**f**) Tumor vessel density was determined by CD31 quantification. Results obtained from six independent pictures for each condition are expressed as mean ± s.e.m. $^*P < 0.05$ compared with the corresponding Scramble clone (ANOVA with Scheffé's test).

Wolfgang Goethe-Universität. Cells were cultured as previously described.[1,68,69]

For HPX, cells were incubated as previously described.[5]

Transfections

Transfections with lipofectamine reagent were performed following the manufacturer's indications. Stable clones were obtained as described,[70] transfecting RCC 786-O cells with pcDNA3-Flag-VHL-shScramble/shRSUME or Flag-VHL L188V-shScramble/shRSUME. pVHL and RSUME expression levels were checked by WB.

Antibodies

The following antibodies were used: anti-V5 and anti-GST (Abcam, Cambridge, UK); anti-β-actin (C4), anti-GFP (B-2), anti-Ubiquitin (P4D1) (SantaCruz Biotechnologies, Heidelberg, Germany); anti-HIF-1α (Affinity BioReagents, Rockford, IL, USA); anti-Flag (Sigma, St Louis, MO, USA); anti-HA (C11) (Covance, Madison, WI, USA), anti-pVHL (BD Pharmigen, Heidelberg, Germany); anti-HIF2α (Novus Biologicals, Cambrigde, UK); anti-VEGF-A and anti-CD31 (PECAM) (R&D Systems, Abingdon, UK); anti-RSUME previously described.[1]

Luciferase assay

Cells were harvested and luciferase activity was measured as previously described.[1,5]

Co-immunoprecipitation

Cells were washed with PBS, lysed on ice with modified RIPA buffer and immunoprecipitated with the indicated antibodies as described.[71] WB analyses were performed with the indicated antibodies.

Tandem immunoprecipitation

Cells were washed with PBS, lysed on ice with modified RIPA buffer and immunoprecipitated with anti-FLAG antibodies as described.[71] Immunoprecipitates were eluted using commercial FLAG peptide (Sigma). Eluates were subjected to a second immunoprecipitation (Tandem immunoprecipitation) using anti-V5 antibodies as described.[71] WB analyses were performed with the indicated antibodies.

Preparation of recombinant proteins

Recombinant proteins were prepared as described.[1,4] Protein expression was confirmed by WB.

GST-ODD hydroxylation

COS-7 cells were lysed as described.[72] 20 μg of recombinant GST-ODD or GST were incubated with COS-7 supernatant, washed with iced buffers B and A and incubated with buffer A, as described.[72]

GST pull-down assay

GST pull down was performed as described,[1,5] incubating 2.5 μg of GST or pVHL-GST fusion proteins with 7.5 μg of His-RSUME recombinant protein.

6xHis-SUMO-2 conjugates purification

6xHis-SUMO-2 conjugates purification was performed as described.[4] Eluates were analyzed by WB.

In vitro ubiquitination assays

In vitro ubiquitination was assayed as described.[73] Briefly, hydroxylated GST or GST-ODD (3 μg) were incubated in the presence of transfected COS-7 cell extracts, in a reaction volume of 20–30 μl for 1–2 h at 30 °C.

In vitro SUMO conjugation assays

SUMO conjugation assays were performed as described[1] following the manufacturer's instructions using the sumoylation kit from LAE Biotech International (Rockville, MD, USA).

Tumors

Human pheochromocytoma and hemangioblastomas explants were obtained from the Center for Endocrinological Investigations, Hospital de Niños R. Gutiérrez, Buenos Aires. Tumors were shock frozen and stored at −80 °C. Samples were used for mRNA isolation for reverse transcription–PCR (RT–PCR) assays or for RSUME protein expression analysis by WB. Formalin-fixed paraffin-embedded human hemangioblastoma was analyzed for RSUME expression by immunofluorescence. This study complies with the June 1964 Declaration of Helsinki, has been approved by the local ethics committee and informed written consent was received from each patient whose tumor tissue was used.

Reverse transcription–PCR

RT–PCR was performed as previously described.[71] PCR was performed with the specific primers: human GAPDH upper primer: 5′-TGAAGGTCGGAGTC AACGGATTTGGT-3′; human GAPDH lower primer: 5′-CATGTGGGCCATG AGGTCCACCAC-3′, PCR product length 948 bp; human RSUME upper primer: 5′-ATGGATCCGCCATGGCGGAGCCTGTGCAGGAGGAG-3′; human RSUME lower primer: 5′-CGTCTAGAATACTTTTTGGCACCTTGAGGTTGTT-3′; PCR product length of 590 bp; human β-actin upper primer: 5′-TGGGCC GCTCTAGGCACCA-3′; human β-actin lower primer: 5′-CGGTTGGCCTTAG GGTTCAGGGGGG-3′; PCR product length 245 bp.

Quantitative real-time RT–PCR was performed with cDNA samples of COS-7 cells as templates. The amplification reactions of 40 cycles were carried out with specific primers for RSUME (upper: 5′-GAGCCGC TCAGAGACAGATG-3′; lower: 5′-TGACTGGCAAATGGAACACC-3′) and Hypoxanthine-guanine phosphoribosyltransferase (HPRT) (upper: 5′- CTCC GTTATGGCGACCCGCAG-3′; lower: 5′-GGCTACAATGTGATGGCCTCCCA-3′). SYBR Green qPCR amplifications were performed in a Bio-Rad Real-time PCR, and the data were analyzed with Bio-Rad CFX Manager software (Bio-Rad, Hercules, CA, USA). For each sample, the values were normalized by the amount of HPRT. All experiments were carried out in triplicates.

Xenograft assay in nude mice

RCC 786-O-derived clones (RCC-786-O, pVHL WT-shScramble, pVHL WT-shRSUME, pVHL L188V-shScramble and pVHL L188V-shRSUME) were collected, washed twice with PBS, resuspended in Dulbecco's Modified Eagle's medium and injected (5×10^6 cells), as described,[71] into the flanks of 6- to 8-week-old male nude mice (strain N:NIH (S)-*Foxn1*^{nu}), obtained from Fundacion Facultad de Ciencias Veterinarios, National University of La Plata, Argentina. Animals were examined for tumor formation every 3 days and tumor growth was measured as described.[71] All experimental protocols were approved by the Ethical Committee on Animal Care and Use (CICUAL), University of Buenos Aires, Argentina.

Immunofluorescence

Five-micrometer sections of shock-frozen RCC tumor tissues were cut by cryostat, fixed with 4% paraformaldehyde in PBS. Tumor slides were incubated (4 °C, 18 h) with antibodies against HIF2α and VEGF-A. Nuclei were stained by 4′,6-diamidino-2-phenylindole. Immunoreactive signals were visualized with appropriate secondary antibodies (Alexa-488 or Alexa-594). Images were acquired with an Carl-Zeiss (Axioskop 2) confocal microscope using a ×60 lens, using AxioCam (MRc5) camera (Carl-Zeiss, Jena, Germany) and Axio Vision Rel 4.4software (Carl-Zeiss). Images were analyzed in ImageJ. HIF-2α and VEGF-A were quantified and normalized to 4′,6-diamidino-2-phenylindole. Six fields were analyzed in each tumor.

Four-micrometer sections of paraffin-embedded human hemangioblastoma were deparaffinized, rehydrated and incubated with anti-RSUME antibody (4 °C, 18 h). After washing with PBS, samples were incubated with secondary antibody Alexa Flour 647 (45 min, room temperature). Nuclei were stained with 4′,6-diamidino-2-phenylindole. Samples were mounted with Mowiol mounting medium. Images were captured by a LSM 710 AxioObserver confocal microscope (Carl-Zeiss). Images were analyzed with ZEN 2011 software (Carl-Zeiss).

Immunohistochemistry

Tumor slides were incubated overnight at 4 °C with CD31 antibody (1:500). After washing, biotinylated horse anti-goat secondary antibody (1:300) was added (room temperature, 30 min). The slides were incubated for 30 min with the avidin–biotin–peroxidase complex (Vector Laboratories Inc., Lörrach, Germany). Color development was performed using 1 mg/ml diaminobenzidine with 0.01% hydrogen peroxide for 8 s. The sections were

counterstained with toluidine blue. Images were acquired at a magnification ×40. Both single cells and cell clusters positive for CD31 were quantified by using ImageJ. Six fields were analyzed in each tumor.

Statistics

Statistics were performed by analysis of variance in combination with the Scheffé's test. Data are shown as mean ± s.e.m.

CONFLICT OF INTEREST

The authors declare no conflict of interest.

ACKNOWLEDGEMENTS

We thank Sergio Senin, María Antunica Noguerol, Jimena Druker and Mariana Haedo for technical help. We also thank the Argentinian Instituto Nacional del Cáncer (INC) and Bunge&Born Foundation for financial support to Lucas Tedesco and Juan Jose Bonfiglio, respectively. This work was supported by grants from the Max Planck Society, Germany; the University of Buenos Aires; CONICET; the Agencia Nacional de Promoción Cientifica y Tecnológica, Argentina and FOCEM-Mercosur (COF 03/11).

REFERENCES

1 Carbia-Nagashima A, Gerez J, Perez-Castro C, Paez-Pereda M, Silberstein S, Stalla GK *et al.* RSUME, a small RWD-containing protein, enhances SUMO conjugation and stabilizes HIF-1alpha during hypoxia. *Cell* 2007; **131**: 309–323.
2 Geiss-Friedlander R, Melchior F. Concepts in sumoylation: a decade on. *Nat Rev Mol Cell Biol* 2007; **8**: 947–956.
3 Hay RT. SUMO: a history of modification. *Mol Cell* 2005; **18**: 1–12.
4 Druker J, Liberman AC, Antunica-Noguerol M, Gerez J, Paez-Pereda M, Rein T *et al.* RSUME enhances glucocorticoid receptor SUMOylation and transcriptional activity. *Mol Cell Biol* 2013; **33**: 2116–2127.
5 Gerez J, Fuertes M, Tedesco L, Silberstein S, Sevlever G, Paez-Pereda M *et al. In silico* structural and functional characterization of the RSUME splice variants. *PLoS One* 2013; **8**: e57795.
6 Huang CC, Tu SH, Lien HH, Jeng JY, Huang CS, Huang CJ *et al.* Concurrent gene signatures for han chinese breast cancers. *PLoS ONE* 2013; **8**: e76421.
7 Schneider BP, Li L, Miller K, Flockhart D, Radovich M, Hancock BA *et al.* Genetic associations with taxane-induced neuropathy by a genome-wide association study (GWAS) in E5103. *J Clin Oncol* 2011; **29**: Supplementary Abstract 1000.
8 Bergmann TK, Vach W, Feddersen S, Eckhoff L, Green H, Herrstedt J *et al.* GWAS-based association between RWDD3 and TECTA variants and paclitaxel induced neuropathy could not be confirmed in Scandinavian ovarian cancer patients. *Acta Oncol* 2013; **52**: 871–874.
9 Rojewska E, Korostynski M, Przewlocki R, Przewlocka B, Mika J. Expression profiling of genes modulated by minocycline in a rat model of neuropathic pain. *Mol Pain* 2014; **10**: 47.
10 Willi-Monnerat S, Migliavacca E, Surdez D, Delorenzi M, Luthi-Carter R, Terskikh AV. Comprehensive spatiotemporal transcriptomic analyses of the ganglionic eminences demonstrate the uniqueness of its caudal subdivision. *Mol Cell Neurosci* 2008; **37**: 845–856.
11 Semenza GL. Regulation of mammalian O2 homeostasis by hypoxia-inducible factor 1. *Annu Rev Cell Dev Biol* 1999; **15**: 551–578.
12 Brahimi-Horn MC, Pouyssegur J. HIF at a glance. *J Cell Sci* 2009; **122**: 1055–1057.
13 Kaelin WG Jr., Ratcliffe PJ. Oxygen sensing by metazoans: the central role of the HIF hydroxylase pathway. *Mol Cell* 2008; **30**: 393–402.
14 Keith B, Johnson RS, Simon MC. HIF1alpha and HIF2alpha: sibling rivalry in hypoxic tumour growth and progression. *Nat Rev Cancer* 2012; **12**: 9–22.
15 Pugh CW, O'Rourke JF, Nagao M, Gleadle JM, Ratcliffe PJ. Activation of hypoxia-inducible factor-1; definition of regulatory domains within the alpha subunit. *J Biol Chem* 1997; **272**: 11205–11214.
16 Berra E, Pouyssegur J. The silencing approach of the hypoxia-signaling pathway. *Methods Enzymol* 2007; **435**: 107–121.
17 Greer SN, Metcalf JL, Wang Y, Ohh M. The updated biology of hypoxia-inducible factor. *EMBO J* 2012; **31**: 2448–2460.
18 Kaelin WG Jr. Molecular basis of the VHL hereditary cancer syndrome. *Nat Rev Cancer* 2002; **2**: 673–682.
19 Yu F, White SB, Zhao Q, Lee FS. HIF-1alpha binding to VHL is regulated by stimulus-sensitive proline hydroxylation. *Proc Natl Acad Sci USA* 2001; **98**: 9630–9635.
20 Schwartz AL, Ciechanover A. Targeting proteins for destruction by the ubiquitin system: implications for human pathobiology. *Annu Rev Pharmacol Toxicol* 2009; **49**: 73–96.
21 Semenza GL. Oxygen sensing, homeostasis, and disease. *N Engl J Med* 2011; **365**: 537–547.
22 Nunez-O'Mara A, Berra E. Deciphering the emerging role of SUMO conjugation in the hypoxia-signaling cascade. *Biol Chem* 2013; **394**: 459–469.
23 Kim WY, Kaelin WG. Role of VHL gene mutation in human cancer. *J Clin Oncol* 2004; **22**: 4991–5004.
24 Maher ER, Kaelin WG Jr. von Hippel-Lindau disease. *Medicine (Baltimore)* 1997; **76**: 381–391.
25 Keefe SM, Nathanson KL, Rathmell WK. The molecular biology of renal cell carcinoma. *Semin Oncol* 2013; **40**: 421–428.
26 Jonasch E, Futreal PA, Davis IJ, Bailey ST, Kim WY, Brugarolas J *et al.* State of the science: an update on renal cell carcinoma. *Mol Cancer Res* 2012; **10**: 859–880.
27 Ohh M, Park CW, Ivan M, Hoffman MA, Kim TY, Huang LE *et al.* Ubiquitination of hypoxia-inducible factor requires direct binding to the beta-domain of the von Hippel-Lindau protein. *Nat Cell Biol* 2000; **2**: 423–427.
28 Kaelin WG Jr. The von Hippel-Lindau tumour suppressor protein: O2 sensing and cancer. *Nat Rev Cancer* 2008; **8**: 865–873.
29 Bae SH, Jeong JW, Park JA, Kim SH, Bae MK, Choi SJ *et al.* Sumoylation increases HIF-1alpha stability and its transcriptional activity. *Biochem Biophys Res Commun* 2004; **324**: 394–400.
30 Cheng J, Kang X, Zhang S, Yeh ET. SUMO-specific protease 1 is essential for stabilization of HIF1alpha during hypoxia. *Cell* 2007; **131**: 584–595.
31 Kim WY, Safran M, Buckley MR, Ebert BL, Glickman J, Bosenberg M *et al.* Failure to prolyl hydroxylate hypoxia-inducible factor alpha phenocopies VHL inactivation *in vivo*. *EMBO J* 2006; **25**: 4650–4662.
32 Cai Q, Verma SC, Kumar P, Ma M, Robertson ES. Hypoxia inactivates the VHL tumor suppressor through PIASy-mediated SUMO modification. *PLoS ONE* 2010; **5**: e9720.
33 Chien W, Lee KL, Ding LW, Wuensche P, Kato H, Doan NB *et al.* PIAS4 is an activator of hypoxia signalling via VHL suppression during growth of pancreatic cancer cells. *Br J Cancer* 2013; **109**: 1795–1804.
34 Rathmell WK, Hickey MM, Bezman NA, Chmielecki CA, Carraway NC, Simon MC. *In vitro* and *in vivo* models analyzing von Hippel-Lindau disease-specific mutations. *Cancer Res* 2004; **64**: 8595–8603.
35 Rechsteiner MP, von Teichman A, Nowicka A, Sulser T, Schraml P, Moch H. VHL gene mutations and their effects on hypoxia inducible factor HIFalpha: identification of potential driver and passenger mutations. *Cancer Res* 2011; **71**: 5500–5511.
36 Hacker KE, Lee CM, Rathmell WK.. VHL type 2B mutations retain VBC complex form and function. *PLoS ONE* 2008; **3**: e3801.
37 Skuli N, Majmundar AJ, Krock BL, Mesquita RC, Mathew LK, Quinn ZL *et al.* Endothelial HIF-2alpha regulates murine pathological angiogenesis and revascularization processes. *J Clin Invest* 2012; **122**: 1427–1443.
38 Kang X, Li J, Zou Y, Yi J, Zhang H, Cao M *et al.* PIASy stimulates HIF1alpha SUMOylation and negatively regulates HIF1alpha activity in response to hypoxia. *Oncogene* 2010; **29**: 5568–5578.
39 van Hagen M, Overmeer RM, Abolvardi SS, Vertegaal AC. RNF4 and VHL regulate the proteasomal degradation of SUMO-conjugated Hypoxia-Inducible Factor-2alpha. *Nucleic Acids Res* 2010; **38**: 1922–1931.
40 Cimarosti H, Lindberg C, Bomholt SF, Ronn LC, Henley JM. Increased protein SUMOylation following focal cerebral ischemia. *Neuropharmacology* 2008; **54**: 280–289.
41 Yang W, Sheng H, Warner DS, Paschen W. Transient focal cerebral ischemia induces a dramatic activation of small ubiquitin-like modifier conjugation. *J Cereb Blood Flow Metab* 2008; **28**: 892–896.
42 Huang C, Han Y, Wang Y, Sun X, Yan S, Yeh ET *et al.* SENP3 is responsible for HIF-1 transactivation under mild oxidative stress via p300 de-SUMOylation. *EMBO J* 2009; **28**: 2748–2762.
43 Shan B, Gerez J, Haedo M, Fuertes M, Theodoropoulou M, Buchfelder M *et al.* RSUME is implicated in HIF-1-induced VEGF-A production in pituitary tumour cells. *Endocr Relat Cancer* 2012; **19**: 13–27.
44 Cerami E, Gao J, Dogrusoz U, Gross BE, Sumer SO, Aksoy BA *et al.* The cBio cancer genomics portal: an open platform for exploring multidimensional cancer genomics data. *Cancer Discov* 2012; **2**: 401–404.
45 Gao J, Aksoy BA, Dogrusoz U, Dresdner G, Gross B, Sumer SO *et al.* Integrative analysis of complex cancer genomics and clinical profiles using the cBioPortal. *Sci Signal* 2013; **6**: pl1.
46 Cancer Genome Atlas Research Network, Comprehensive molecular characterization of clear cell renal cell carcinoma. *Nature* 2013; **499**: 43–49.
47 Hoffman MA, Ohh M, Yang H, Klco JM, Ivan M, Kaelin WG Jr. von Hippel-Lindau protein mutants linked to type 2C VHL disease preserve the ability to downregulate HIF. *Hum Mol Genet* 2001; **10**: 1019–1027.

48 Knauth K, Bex C, Jemth P, Buchberger A. Renal cell carcinoma risk in type 2 von Hippel-Lindau disease correlates with defects in pVHL stability and HIF-1alpha interactions. *Oncogene* 2006; **25**: 370–377.
49 Semenza GL. HIF-1 mediates metabolic responses to intratumoral hypoxia and oncogenic mutations. *J Clin Invest* 2013; **123**: 3664–3671.
50 Knauth K, Cartwright E, Freund S, Bycroft M, Buchberger A. VHL mutations linked to type 2C von Hippel-Lindau disease cause extensive structural perturbations in pVHL. *J Biol Chem* 2009; **284**: 10514–10522.
51 Rathmell WK, Godley PA. Recent updates in renal cell carcinoma. *Curr Opin Oncol* 2010; **22**: 250–256.
52 Cowey CL, Rathmell WK. VHL gene mutations in renal cell carcinoma: role as a biomarker of disease outcome and drug efficacy. *Curr Oncol Rep* 2009; **11**: 94–101.
53 Brooks SA, Brannon AR, Parker JS, Fisher JC, Sen O, Kattan MW *et al.* ClearCode34: A prognostic risk predictor for localized clear cell renal cell carcinoma. *Eur Urol* 2014; **66**: 77–84.
54 Gnarra JR, Zhou S, Merrill MJ, Wagner JR, Krumm A, Papavassiliou E *et al.* Post-transcriptional regulation of vascular endothelial growth factor mRNA by the product of the VHL tumor suppressor gene. *Proc Natl Acad Sci USA* 1996; **93**: 10589–10594.
55 Iliopoulos O, Kibel A, Gray S, Kaelin WG Jr. Tumour suppression by the human von Hippel-Lindau gene product. *Nat Med* 1995; **1**: 822–826.
56 Zimmer M, Doucette D, Siddiqui N, Iliopoulos O. Inhibition of hypoxia-inducible factor is sufficient for growth suppression of VHL-/- tumors. *Mol Cancer Res* 2004; **2**: 89–95.
57 Maranchie JK, Vasselli JR, Riss J, Bonifacino JS, Linehan WM, Klausner RD. The contribution of VHL substrate binding and HIF1-alpha to the phenotype of VHL loss in renal cell carcinoma. *Cancer Cell* 2002; **1**: 247–255.
58 Richard DE, Berra E, Pouyssegur J. Nonhypoxic pathway mediates the induction of hypoxia-inducible factor 1alpha in vascular smooth muscle cells. *J Biol Chem* 2000; **275**: 26765–26771.
59 Tanos T, Marinissen MJ, Leskow FC, Hochbaum D, Martinetto H, Gutkind JS *et al.* Phosphorylation of c-Fos by members of the p38 MAPK family. Role in the AP-1 response to UV light. *J Biol Chem* 2005; **280**: 18842–18852.
60 Groulx I, Lee S. Oxygen-dependent ubiquitination and degradation of hypoxia-inducible factor requires nuclear-cytoplasmic trafficking of the von Hippel-Lindau tumor suppressor protein. *Mol Cell Biol* 2002; **22**: 5319–5336.
61 Safran M, Kim WY, O'Connell F, Flippin L, Gunzler V, Horner JW *et al.* Mouse model for noninvasive imaging of HIF prolyl hydroxylase activity: assessment of an oral agent that stimulates erythropoietin production. *Proc Natl Acad Sci USA* 2006; **103**: 105–110.
62 Kondo K, Klco J, Nakamura E, Lechpammer M, Kaelin WG Jr. Inhibition of HIF is necessary for tumor suppression by the von Hippel-Lindau protein. *Cancer Cell* 2002; **1**: 237–246.
63 Post DE, Van Meir EG. Generation of bidirectional hypoxia/HIF-responsive expression vectors to target gene expression to hypoxic cells. *Gene Ther* 2001; **8**: 1801–1807.
64 Schoenfeld AR, Davidowitz EJ, Burk RD. Elongin BC complex prevents degradation of von Hippel-Lindau tumor suppressor gene products. *Proc Natl Acad Sci USA* 2000; **97**: 8507–8512.
65 Desterro JM, Rodriguez MS, Hay RT. SUMO-1 modification of IkappaBalpha inhibits NF-kappaB activation. *Mol Cell* 1998; **2**: 233–239.
66 Tatham MH, Jaffray E, Vaughan OA, Desterro JM, Botting CH, Naismith JH *et al.* Polymeric chains of SUMO-2 and SUMO-3 are conjugated to protein substrates by SAE1/SAE2 and Ubc9. *J Biol Chem* 2001; **276**: 35368–35374.
67 Rodriguez MS, Dargemont C, Hay RT. SUMO-1 conjugation *in vivo* requires both a consensus modification motif and nuclear targeting. *J Biol Chem* 2001; **276**: 12654–12659.
68 Juengel E, Engler J, Natsheh I, Jones J, Mickuckyte A, Hudak L *et al.* Combining the receptor tyrosine kinase inhibitor AEE788 and the mammalian target of rapamycin (mTOR) inhibitor RAD001 strongly inhibits adhesion and growth of renal cell carcinoma cells. *BMC Cancer* 2009; **9**: 161.
69 Lolkema MP, Gervais ML, Snijckers CM, Hill RP, Giles RH, Voest EE *et al.* Tumor suppression by the von Hippel-Lindau protein requires phosphorylation of the acidic domain. *J Biol Chem* 2005; **280**: 22205–22211.
70 Castro CP, Giacomini D, Nagashima AC, Onofri C, Graciarena M, Kobayashi K *et al.* Reduced expression of the cytokine transducer gp130 inhibits hormone secretion, cell growth, and tumor development of pituitary lactosomatotrophic GH3 cells. *Endocrinology* 2003; **144**: 693–700.
71 Paez-Pereda M, Giacomini D, Refojo D, Nagashima AC, Hopfner U, Grubler Y *et al.* Involvement of bone morphogenetic protein 4 (BMP-4) in pituitary prolactinoma pathogenesis through a Smad/estrogen receptor crosstalk. *Proc Natl Acad Sci USA* 2003; **100**: 1034–1039.
72 Huang J, Zhao Q, Mooney SM, Lee FS. Sequence determinants in hypoxia-inducible factor-1alpha for hydroxylation by the prolyl hydroxylases PHD1, PHD2, and PHD3. *J Biol Chem* 2002; **277**: 39792–39800.
73 Cockman ME, Masson N, Mole DR, Jaakkola P, Chang GW, Clifford SC *et al.* Hypoxia inducible factor-alpha binding and ubiquitylation by the von Hippel-Lindau tumor suppressor protein. *J Biol Chem* 2000; **275**: 25733–25741.

Supplementary Information accompanies this paper on the Oncogene website (http://www.nature.com/onc)